Cancer Chemotherapy and Pharmacology (2019) 84:1241–1256
https://doi.org/10.1007/s00280-019-03962-8

ORIGINAL ARTICLE

Dasatinib attenuates overexpression of Src signaling induced by the combination treatment of veliparib plus carboplatin in triple-negative breast cancer

Yuliang Sun[1] · Xiaoqian Lin[1] · Jennifer Carlson Aske[1] · Ping Ye[1] · Casey Williams[1] · Mark Abramovitz[1] · Brian R. Leyland-Jones[1]

Received: 4 April 2019 / Accepted: 11 September 2019 / Published online: 20 September 2019

Abstract

Purpose Triple-negative breast cancer (TNBC) has a poor prognosis because of limited treatment options. The combination of a poly ADP ribose polymerase (PARP) inhibitor with a DNA-damaging agent has shown promise in treating TNBC; however, not all patients respond to this combination. The Src protein kinase modulates multiple cancer cell properties and plays a key role in tumorigenic processes. However, Src inhibitors as single agents have shown limited effects in solid tumors. Here, we examined the antitumor effects of the Src inhibitor dasatinib, the PARP inhibitor veliparib, and the DNA-damaging agent carboplatin in TNBC models to try and identify the combination with the most clinical potential.

Methods Dasatinib, veliparib and carboplatin were tested in TNBC cells in vitro and in xenograft tumors in vivo.

Results Surprisingly, treatment with the combination of veliparib plus carboplatin led to an increase in Src phosphorylation. Importantly, dasatinib attenuated Src overexpression induced by veliparib plus carboplatin and further inhibited the downstream signaling of Src. In xenograft models, the triple combination of dasatinib with veliparib plus carboplatin showed greater tumor growth inhibitory effects compared with single agents or double combinations. No systemic toxicity was observed in mice treated with the triple combination.

Conclusions This study emphasizes the merit of evaluating the triple combination therapy, dasatinib with veliparib plus carboplatin, in TNBC clinical trials.

Keywords Src · Dasatinib · Veliparib · Carboplatin · Triple-negative breast cancer

Abbreviations

TNBC	Triple-negative breast cancer
PARP	Poly ADP ribose polymerase
HR	Homologous recombination
IHC	Immunohistochemistry
pCR	Pathological complete response

Introduction

Breast cancer is a heterogeneous disease with different molecular phenotypes, clinical features, and responses to treatment [1–3]. TNBC accounts for approximately 15–20% of diagnosed breast cancers and depends on the accurate assessment of the status of the estrogen receptor (ER), progesterone receptor (PR), and human epidermal growth factor receptor 2 (HER2) [4]. Although the identification of gene mutations and signaling pathways over the past decades has facilitated a major effort to discover actionable molecular targets in TNBC for drug development, chemotherapy remains the standard of care in patients with TNBC in both the early and advanced stages of the disease [5]. Therefore, development of new molecular targeted drugs and of optimal therapeutic strategies for the treatment of TNBC is urgently needed.

In recent studies, DNA repair systems have emerged as molecular targets in cancer with *BRCA1/2* mutations. *BRCA*

Electronic supplementary material The online version of this article (https://doi.org/10.1007/s00280-019-03962-8) contains supplementary material, which is available to authorized users.

✉ Yuliang Sun
Yuliangsun2@gmail.com

✉ Brian R. Leyland-Jones
BleylandJ@aol.com

[1] Avera Center for Precision Oncology, Avera Cancer Institute, Sioux Falls, 1000 E 23rd St., Sioux Falls, SD 57105, USA

germline mutations are found in approximately 10–20% of TNBC patients, resulting in somatic deficiencies in homologous recombination (HR), the so-called "*BRCA*ness" phenotype [6]. Proteins encoded by *BRCA1/2* function at different stages in the DNA damage response (DDR) and in DNA repair [7]. PARP produces poly (ADP ribose) (PAR) that plays an important role in DNA repair, cell differentiation, chromosomal instability, and gene regulation [8]. *BRCA1/2*-deficient cells show increasing sensitivity to PARP inhibitors [9], and a proof-of-concept trial provided a favorable therapeutic index for PARP inhibition in advanced breast cancer patients with *BRCA1* or *BRCA2* mutations [10].

Several PARP inhibitors are currently being evaluated in clinical trials in TNBC patients with a deficient HR pathway. The phase 3 OlympiAD trial, in which a PARP inhibitor (olaparib) was compared with physician's choice chemotherapy in the treatment of metastatic germline *BRCA*-mutated breast cancer patients, reported a significant improvement in median progression-free survival (PFS) in patients treated with the PARP inhibitor [11]. Conversely, since there are poor responses in *BRCA*-proficient tumors to monotherapy with PARP inhibitors, appropriate therapies in the future could involve the combination of PARP inhibition with cytotoxic DNA-damaging agents and/or with molecular targeted agents.

Our previous preclinical study showed that the combination of a PARP inhibitor (veliparib) with carboplatin resulted in better in vivo antitumor effects compared with veliparib or carboplatin as single agents in TNBC xenograft models with or without a *BRCA*-mutation [12]. More recently, PARP inhibitors have shown potential in increasing the sensitivity of tumor cells to platinum-based agents and providing a therapeutic benefit to patients with advanced malignancies, whether they had mutations in *BRCA* or DNA repair pathway genes. However, over 40% of patients did not have a pathological complete response (pCR) to the combination [13–15].

Src family kinases (SFKs) are non-receptor tyrosine kinases that include Src and Lyn, which have been implicated in oncogenesis. SFKs regulate multiple cancer cell processes including cell cycle progression, survival, and metastasis [16]. Elevated Src protein activity has been shown to lead resistance to PI3 K inhibitors [17], whereas PI3K inhibition sensitizes TNBC to PARP inhibitor [18].

Dasatinib is an orally active small molecule inhibitor of both the Src and Abl proteins that is currently approved for the treatment of acute lymphoblastic leukemia (ALL) and chronic myelogenous leukemia (CML). Dasatinib has also shown activity against epithelial tumor cells, including human ovarian, lung, and breast cancer cells [19]. However, in a phase 2 clinical trial in which dasatinib was administered as a monotherapy, it failed to demonstrate significant efficacy in TNBC patients [19, 20]. The use of Src inhibitors in novel combinations may enhance their therapeutic potential. Dasatinib has been reported to increase the sensitivity of ovarian cancer to carboplatin and the combination was safe [21]. Currently, clinical trials in TNBC patients are underway that employ dasatinib as a single agent (NCT01471106) or in combination with other drugs (NCT01015222). Taken together, the properties of dasatinib make it a promising component of multi-drug regimens when combined with PARP inhibitors plus cytotoxic agents [17, 18, 21, 22].

In this study, we evaluated dasatinib, veliparib, and carboplatin as single agents, in double combinations, and as a triple combination in TNBC cells in vitro and in tumors in vivo. We studied the effects of these agents on Src activity in TNBC cell lines and on tumor growth in mouse xenograft models. Here, we provide novel evidence that veliparib combined with carboplatin drives Src activation in the preclinical models tested. Moreover, we provide provocative in vitro and in vivo data indicating the potential for increasing therapeutic efficacy by combining dasatinib with veliparib and carboplatin in TNBC.

Materials and methods

Antibodies and reagents

Antibodies against p-AKT^{S473}, p-AKT^{T308}, AKT, cleaved caspase 3^{Asp175}, caspase 3, p-ERK$^{T202/Y204}$, ERK, Ki-67, p27^{Kip1}, cleaved PARP^{Asp214}, PARP, pS6 RP$^{S235–236}$, S6 RP, p-Src^{Y416}, p-Src^{Y527}, and Src (Cell Signaling Technology, Danvers, MA, USA), and CD31, cyclin D1, and beta-actin (Abcam, Cambridge, MA, USA) were used in the study. Dasatinib and veliparib were kindly supplied by the National Cancer Institute (NCI, Bethesda, MD, USA) and PP2 was purchased from Selleck Chemicals (Houston, TX, USA). In vivo studies were carried out using dasatinib and veliparib purchased from Selleck Chemicals, and carboplatin was purchased from the Avera McKennan Hospital Pharmacy (Sioux Falls, SD, USA). All common reagents were obtained from Thermo Fisher Scientific (Waltham, MA, USA) or Sigma-Aldrich (St. Louis, MO, USA).

Cell lines and cell culture

BT-20, HCC70, HCC1937, MDA-MB-231, and MDA-MB-468 TNBC cell lines and human umbilical vein endothelial cells (HUVEC) were obtained from the American Type Culture Collection (ATCC, Manassas, VA, USA), and the TNBC cell line SUM149PT was procured from Asterand Bioscience Inc. (Cambridge, MA, USA). Cells were cultured according to the standard protocols.

Proliferation assay

Proliferation was determined using the CellTiter 96 Aqueous One Solution Cell Proliferation Assay (MTS) kit (Promega, Madison, WI, USA), as per the manufacturer's protocol. Cells (at least in triplicate) were treated and incubated at 37 °C for 96 h before adding the MTS reagent. Absorbance was assessed at 570 nm using a microplate reader (iMark; Bio-Rad, Hercules, CA, USA).

Cellular apoptotic assay

After treatment, cells were rinsed in PBS and released from wells using trypsin. Cells were resuspended in Annexin V binding buffer and stained with 5% Annexin V-PE and 5% 7AAD (BD Biosciences, Franklin Lakes, NJ, USA). Cells were run in triplicate on an Accuri C6 flow cytometer and BD Accuri C6 software was used to analyze results.

Western blot analysis

For total protein extraction, cells were collected immediately before use in cold lysis buffer containing a protease inhibitor cocktail. Protein concentrations were determined using a Bio-Rad protein assay kit. Equal amounts of protein were resolved on a 4–20% SDS-PAGE (Bio-Rad) and transferred to a nitrocellulose membrane. Membranes were then incubated with the respective antibodies. Beta-actin was used as a loading control [22].

Clonogenic growth assay

The three-dimensional (3D) 'on-top'-colony assay was standardized with little modification from the published protocol [12, 23]. The clonogenic assay was performed for 96 h using matrigel as the matrix. Pictures of live colonies were taken using an Olympus XM10 digital camera.

Tube formation assay

HUVECs were added to the wells containing solidified matrigel (250 µl), treated with compounds, and incubated at 37 °C in 5% CO_2 atmosphere. Photomicrographs were taken at 4, 6, and 18 h [22].

Xenograft model and in vivo treatment response

In vivo efficacy of drug combinations was evaluated in athymic mice bearing established xenograft tumors following Institutional Animal Care and Use Committee (IACUC) guidelines. Cells in saline (5×10^6 MDA-MB-231 cells; 2×10^6 MDA-MB-468 cells; 5×10^6 SUM149PT cells) were suspended in matrigel (50:50) and injected subcutaneously into the flank of immunocompromised female nude (nu/nu) mice (Taconic Farms, Inc., Germantown, NY, USA).

After implantation of cells into mice, tumors were monitored until they reached mean tumor volumes of ~ 200 mm^3 and were distributed into groups of five to eight mice/group (see details in Table 2), ensuring that each group had equivalent mean tumor volumes prior to initiating dosing. Tumor measurements were determined using digital calipers and tumor volume was calculated using the formula $(L \times W^2)/2$, where L and W are the major and minor diameters (in millimeters) and expressed as mean tumor volume (mm^3). Mice with tumor volumes > 2,000 mm^3 or with losses in body weight of 20% or more from their weight at the start of treatment were killed as per institutional IACUC guidelines.

Immunohistochemical analysis (IHC)

Deparaffinized and rehydrated tissue sections were subjected to antigen retrieval using an IHC-Tek Epitope Retrieval Steamer Set (IHC WORLD, Ellicott City, MD, USA) and then incubated in Dual Endogenous Enzyme Block solution (Dako, Carpinteria, CA, USA). To detect specific staining, tissue sections were treated with EnVision + Dual Link System-HRP (DAB +) (Dako). Matched IgG (Dako) was used as a negative control. Image acquisition was performed using an Olympus DP72 camera and CellSens software. Magnification was 400X (scale bars are ~ 20 µm).

Statistical analysis

ANOVA test was employed to compare the mean of each treatment group with the mean of every other group using GraphPad Prism 6 software. P values of < 0.05 were considered statistically significant for all tests.

Results

Sensitivity of TNBC cells to dasatinib as a single agent or in combination with veliparib and/or carboplatin

The goal of the first part of this study was to test the activity of Src in a panel of TNBC cell lines containing mutations in the commonly mutated oncogenes and to compare the inhibitory effect of dasatinib on the growth of TNBC cells. Molecular characteristics of the cell lines are summarized in Table 1. Cells were treated with increasing doses of dasatinib as single agent or with the triple combination of dasatinib (increasing dose) with veliparib (fixed does at 10 µM) and carboplatin (fixed does at 10 µM) for 96 h. Cell growth was quantified using the MTS assay. *KRAS/BRAF-mutated* MDA-MB-231 cells were highly sensitive

Table 1 Proliferation assay results (96 h incubation)

Cell line	Dasatinib IC_{50} (μM ± SD)	Dasatinib IC_{50} (in combination)	*p* value	Molecular characteristics
BT-20	N/A	N/A	N/A	*PIK3CA-mutated*
HCC70	8 ± 0.05	0.3 ± 0.02	< 0.00001	*PTEN* null
HCC1937	0.3 ± 0.02	0.06 ± 0.01	< 0.00005	*BRCA1*-mutated, *PTEN* null
MDA-MB-231	0.07 ± 0.02	0.06 ± 0.01	0.48182	*KRAS/BRAF*-mutated
MDA-MB-468	4 ± 0.06	7 ± 0.02	< 0.00001	*PTEN* null
SUM149PT	3 ± 0.02	0.008 ± 0.00	< 0.00001	*BRCA1*-mutated, *PTEN* null

IC_{50} half maximal inhibitory concentration, *N/A* IC_{50} was not reached, *SD* standard deviation

Dasatinib IC_{50} (in combination): dasatinib (μM) combined with veliparib (10 μM) plus carboplatin (10 μM). Assays were done in triplicate ($n = 3$), all *p* values are from *t*-test using the Holm-Sidak method of GraphPad Prism 6

to dasatinib alone with an IC_{50} of 0.07 μM. Other cell lines were less responsive to dasatinib as a single agent including HCC70, HCC1937, MDA-MB-468, and SUM149PT with IC_{50} values of 8, 0.3, 4, and 3 μM, respectively, whereas an IC_{50} was not reached with *PIK3CA*-mutated BT-20 cells. Interestingly, IC_{50} values for dasatinib in combination with veliparib and carboplatin were notably decreased in HCC1937, SUM149PT, and HCC70 cell lines (0.06, 0.008, and 0.3 μM, respectively). The combination of agents did not enhance the sensitivity of BT-20 cells to dasatinib (Table 1, Supplementary Fig S1).

We next evaluated whether dasatinib was inhibiting Src signaling by western blot analyses. As seen in Fig. 1a, dasatinib effectively inhibited p-Src^{Y416} activity in a dose-dependent manner. We also observed that p-Src^{Y416} inhibition was induced with PP2 (a "selective" Src inhibitor, Fig. 1a). Of note, a similar inhibition of Src phosphorylation has been seen in *PIK3CA-mutated* BT-20 and *PTEN* null HCC70 cells, which were less responsive to dasatinib as a single agent in the MTS assay. This is consistent with previous studies that showed that inhibition of cell proliferation by dasatinib did not correlate with inhibition of Src activity [24]. Based on these results, we selected two concentrations of dasatinib, 10 nM and 50 nM that can induce inhibition of Src activity, for our in vitro studies.

Dasatinib attenuated Src activity caused by veliparib plus carboplatin in vitro and in vivo

Western blotting was conducted to measure total and phosphorylated levels of the Src protein following treatment with dasatinib alone or in combination with veliparib and carboplatin. Surprisingly, veliparib plus carboplatin increased Src^{Y416} phosphorylation in PTEN null HCC70, MDA-MB-468, and *BRCA*-mutated and *PTEN* null HCC1937 cells, as well as in *KRAS/BRAF-mutated* MDA-MB-231 and SUM149PT cells. This increased Src activity was attenuated by adding dasatinib to the combination of veliparib and carboplatin (Fig. 1b). We also investigated the activity of p-Src on Y527, which is an inhibitory phosphorylation site. Interestingly, increased phosphorylation at this site was also induced by veliparib plus carboplatin treatment in HCC70, HCC1937, MDA-MB-231, MDA-MB-468, and SUM149PT cells, and the phosphorylation of Y527 was inhibited by adding dasatinib (Fig. 1b). Our finding was consistent with those of previous reports showing that C-terminal Src kinase of p-Src^{Y527} can be blocked by dasatinib through nonspecific inhibition [16, 25].

To further confirm the in vivo efficacy of dasatinib as a single agent or in combination on Src expression in TNBC, we performed IHC with the anti-p-Src^{Y416} antibody on formalin-fixed, paraffin-embedded (FFPE) tumor sections from xenograft models. Tumors treated with dasatinib alone exhibited a significant decrease in p-Src^{Y416} expression in all three models. The double combination of dasatinib and carboplatin also induced an obvious inhibition of p-Src^{Y416} expression in MDA-MB-231 tumor cells, and further decreases in p-Src^{Y416} expression were observed using the triple combination in all three models. Of note, increases in p-Src^{Y416} expression occurred in *KRAS/BRAF-mutated* MDA-MB-231 tumor cells induced by the combination of veliparib and carboplatin, which was consistent with our in vitro results (Fig. 1c, Supplementary Fig S2**a**).

Combination of dasatinib and veliparib plus carboplatin leads to blockade of oncogenic signaling pathways and inhibits proliferation of TNBC cells in vitro and in vivo

After observing the in vitro and in vivo effects of dasatinib alone or in combination on Src activity, we tested whether dasatinib alone and in combination with veliparib and carboplatin were effective at inhibiting clonogenic survival. Consistent with our MTS results, MDA-MB-231 cells were highly sensitive to dasatinib treatment in the 3-D 'on-top' assay. The greatest effect on blocking colony formation

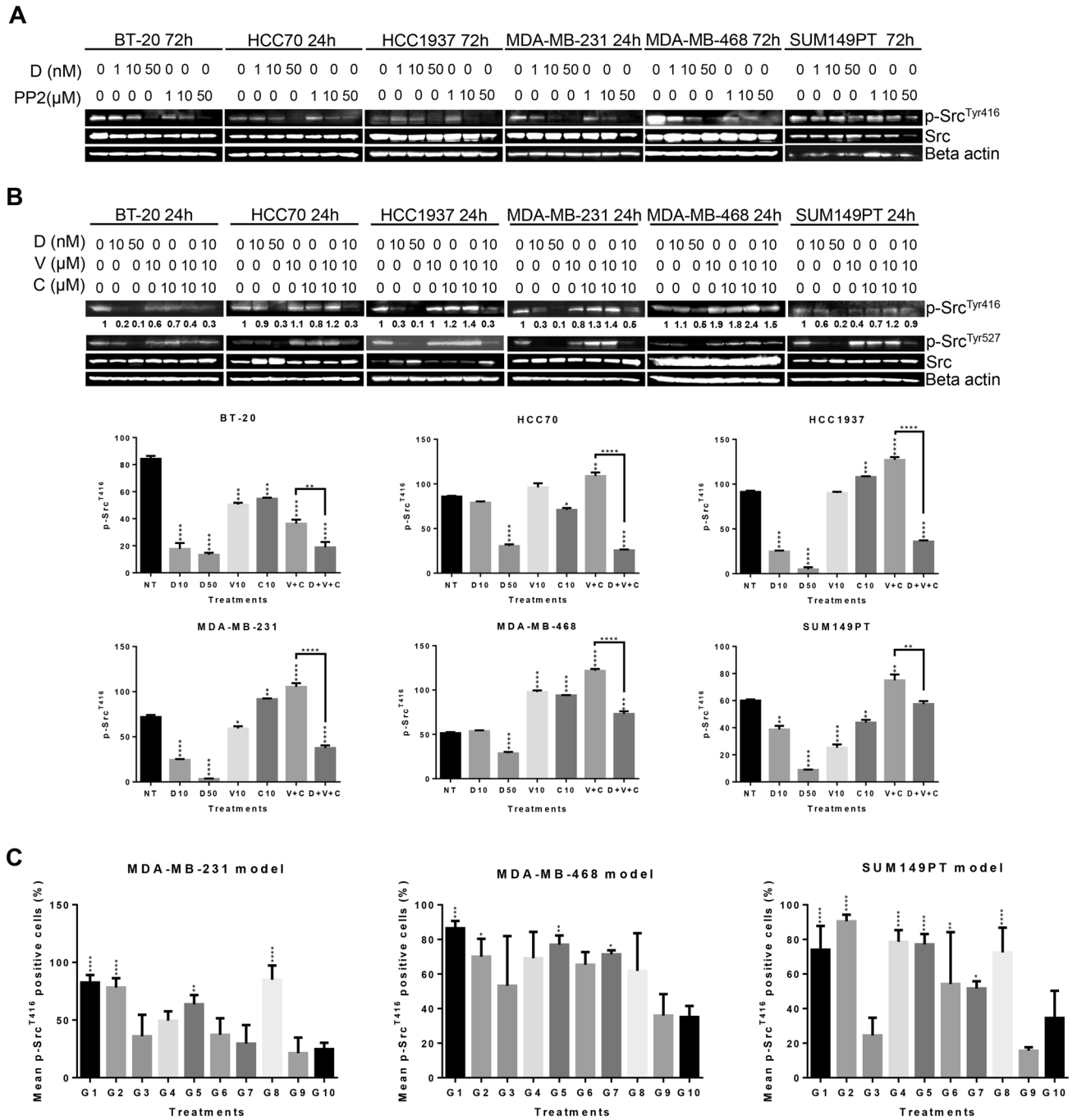

Fig. 1 Effect of dasatinib as a single agent or in combination with veliparib and/or carboplatin on inhibition of Src signaling in TNBC cells in vitro and in vivo. BT-20, HCC70, HCC1937, MDA-MB-231, MDA-MB-468, and SUM149PT cells were starved in 0.1% FBS medium (phenol red free) for 4 h and then: **a** Treated with dasatinib (D) (1, 10, and 50 nM) or PP2 (1, 10, and 50 μM) for 24 or 72 h. Whole cell lysates were immunoblotted with anti-Src and anti-p-Src^{Y416} antibodies. **b** Treated with dasatinib (10 or 50 nM) as a single agent or in combination with veliparib (10 μM) and/or carboplatin (10 μM) for 24 h. Whole cell lysates were immunoblotted with anti-Src, anti-p-Src^{Y416}, and anti-p-Src^{Y527} antibodies. Densitometry results (using VisionWorks Life Science software) of p-Src^{Y416} were calculated as ratios relative to untreated control normalized to beta-actin protein loading control (Numbers below p-Src^{Y416}). Three batches of independently cultured/treated cells are represented for each cell line and each experiment was done in triplicate. Data (compared to no treatment control) were then analyzed using one-way ANOVA followed by Sidak's post hoc test (*, $p<0.05$; ** $p<0.005$; ***, $p<0.001$; ****, $p<0.0001$). **c** In MDA-MB-231, MDA-MB-468, and SUM149PT xenograft tumor tissues, the expression status of phospho-SRC was determined by IHC. After quantification (using OLYMPUS cellSens Standard software), the mean percentage of phospho-SRC positive cells from 4 high-power (x 400) fields is shown graphically, and the bar is SD ($n=4$). *, $p<0.05$; ** $p<0.005$; ***, $p<0.001$; ****, $p<0.0001$ compared the mean of each group with the mean of group 9 (triple combination) by one-way ANOVA followed by Turkey's post hoc test. See details of treatment groups in the legend of Fig. 6

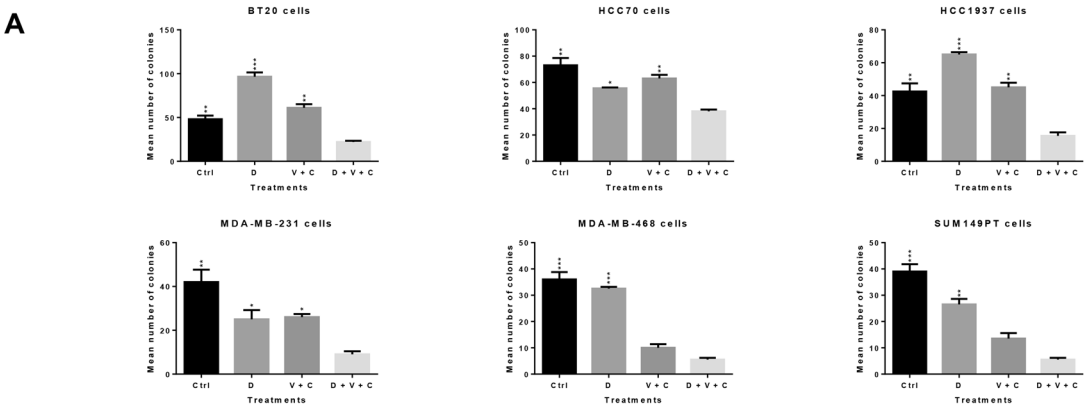
A
BT20 cells
HCC70 cells
HCC1937 cells
MDA-MB-231 cells
MDA-MB-468 cells
SUM149PT cells
Mean number of colonies
Ctrl
D
V + C
D + V + C
Treatments


B
BT-20 24h
HCC70 24h
HCC1937 24h
MDA-MB-231 24h
MDA-MB-468 24h
SUM149PT 24h
D (nM) 0 10 50 0 0 0 10
V (μM) 0 0 0 10 0 10 10
C (μM) 0 0 0 0 10 10 10
p-AKTThr308
p-AKTSer473
AKT
p-S6 RP
S6 RP
p-ERK
ERK
Beta actin

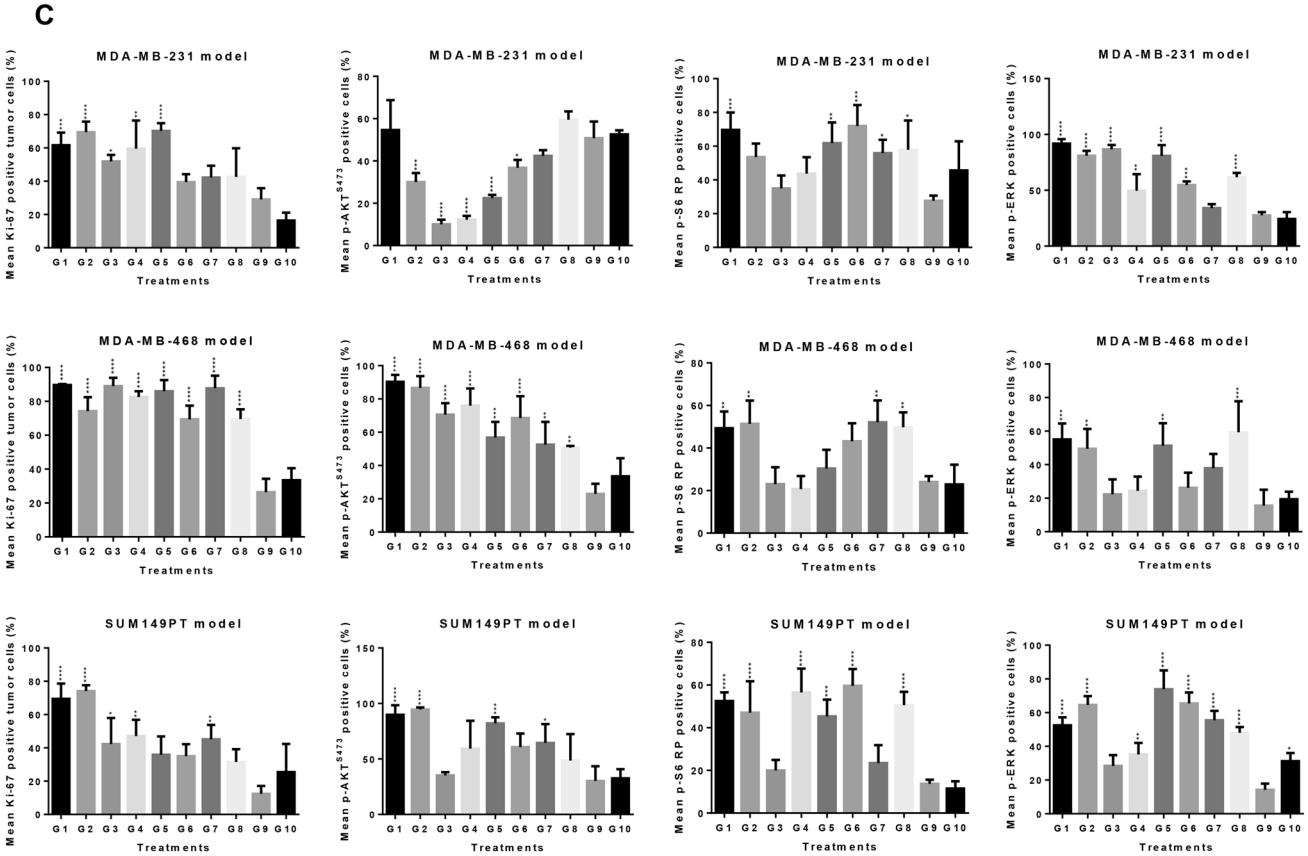
C
MDA-MB-231 model
MDA-MB-468 model
SUM149PT model
Mean Ki-67 positive tumor cells (%)
Mean p-AKTS473 positive cells (%)
Mean p-S6 RP positive cells (%)
Mean p-ERK positive cells (%)
G1 G2 G3 G4 G5 G6 G7 G8 G9 G10
Treatments

◂**Fig. 2** Dasatinib as a single agent or in combination with veliparib and/or carboplatin inhibits tumor cell proliferation/survival signaling in vitro and in vivo. **a** BT-20, HCC70, HCC1937, MDA-MB-231, MDA-MB-468, or SUM149PT cells were seeded on solidified matrigel in the presence and absence of drug for 96 h, and pictures were taken at 100 × magnification using an Olympus XM10 camera. Results are presented as the mean colony number (using VisionWorks Life Science software), and the bar is the SD ($n=2$). *, $p<0.05$; **, $p<0.005$; ***, $p<0.001$ compared the mean of each column with the mean of every other column by one-way ANOVA. Abbreviation: Ctrl, control (no treatment); D, dasatinib; V, veliparib; C carboplatin. **b** BT-20, HCC70, HCC1937, MDA-MB-231, MDA-MB-468, and SUM149PT cells were starved in 0.1% FBS medium (phenol red free) for 4 h and treated with dasatinib (10 or 50 nM) as a single agent or in combination with veliparib (10 μM) and/or carboplatin (10 μM) for 24 h. Whole cell lysates were immunoblotted using anti-AKT, anti-p-AKT^{S473} and anti-p-AKT^{T308}, anti-S6 RP, anti-p-S6 RP$^{S235-236}$, anti-ERK, and anti-p-ERK$^{T202/Y204}$ antibodies. Densitometry results (using VisionWorks Life Science software) of p-AKT^{T308}, p-AKT^{S473} p-ERK and p-S6 RP were calculated as ratios relative to untreated control normalized to beta-actin protein loading control. **c** In MDA-MB-231, MDA-MB-468, and SUM149PT xenograft tumor tissues, the expression status of Ki-67, phospho-AKT^{S473}, p-S6 RP and p-ERK was determined by IHC. After quantification, the mean percentage of positive cells of each staining from 4 high-power (x 400) fields is shown graphically, and the bar is SD ($n=4$). *, $p<0.05$; **, $p<0.005$; ***, $p<0.001$; ****, $p<0.0001$ compared the mean of each group with the mean of group 9 (triple combination) by one-way ANOVA followed by Turkey's post hoc test

across all cell lines was seen in MDA-MB-231 cells. The combination of veliparib and carboplatin also significantly blocked clonogenic survival in all tested cell lines. The triple combination further decreased colony formation in all TNBC cell lines (Fig. 2a, Supplementary Fig S3). Dasatinib alone or in combination was less effective in blocking colony formation in the BT-20 cell line, which was consistent with our previous results.

We next evaluated signaling changes in AKT, S6 ribosomal protein (RP), and ERK pathways in response to the treatments. Dasatinib alone decreased p-AKT^{T308} expression in BT-20, HCC70, and MDA-MB-231 cells, and inhibited p-AKT^{S473} expression in HCC70, HCC1937, and MDA-MB-231 cell lines as well as in SUM149PT cells. Dasatinib alone only blocked S6 RP$^{S235/236}$ phosphorylation in MDA-MB-231 and SUM149PT cells dose dependently, and decreased ERK$^{T202/T204}$ activity in HCC1937, MDA-MB-468, and SUM149PT cells. Cells treated with the triple combination showed a decrease in p-AKT^{T308} and p-AKT^{S473} expression in SUM149PT cells, and a decrease in p-AKT^{S473} expression in HCC1937 cells (Fig. 2b). We also observed inhibition of p-S6 RP$^{S235/236}$ and p-ERK$^{T202/T204}$ expression in MDA-MB-231 and SUM149PT cells using the triple combination. Interestingly, triple combination increased p-AKT^{S473} and p-ERK$^{T202/T204}$ expression in BT-20 cells. This suggests that increased AKT^{S473} and ERK$^{T202/T204}$ activities attenuated the effect of Src inhibition, resulting in less of a response in the MTS and 3D 'on-top' assays.

To more specifically assess the mechanism of action of dasatinib alone or in combination on proliferative/survival signaling in xenograft TNBC tumor cells, expression levels of Ki-67, p-AKT^{S473}, p-S6 RP$^{S235/236}$, and p-ERK$^{T202/T204}$ were determined using IHC on FFPE sections. IHC indicated that compared with vehicle control, treatment with a single agent, dasatinib, veliparib, or carboplatin resulted in (a) slightly decreased cell proliferation (Ki-67) in MDA-MB-231 and MDA-MB-468 tumor cells, and (b) significantly decreased Ki-67 in SUM149PT tumor cells. The double combination of dasatinib plus veliparib, dasatinib plus carboplatin, or veliparib plus carboplatin significantly blocked Ki-67 expression in all three xenograft models. The triple combination resulted in markedly decreased Ki-67 expression in all three TNBC models (Fig. 2c, Supplementary Fig S2b). We observed inhibition of p-AKT^{S473} expression that was induced by treatment with either a single agent or double combinations in all three models, as well as a decrease in p-AKT^{S473} expression induced by the triple combination in MDA-MB-468 and SUM149PT tumor cells. In contrast, there were no changes in p-AKT^{S473} expression in MDA-MB-231 tumor cells treated with the triple combination (Fig. 2c, Supplementary Fig S2e). Furthermore, we observed that p-S6 RP$^{S235/236}$ and p-ERK$^{T202/T204}$ levels were decreased after treatment with a single agent or with double combinations. The best inhibitory effect was observed with the triple combination (Fig. 2c, Supplementary Fig S2f, g).

Combination of dasatinib and veliparib plus carboplatin induces apoptosis in TNBC cells in vitro and in vivo

We next evaluated the mechanism of action of dasatinib alone or in combination on cellular apoptosis by western blotting. Activation of caspase-3^{Asp175}, as exhibited by increased cleaved protein bands at 17 and 19 kDa, was observed after incubation with the triple combination for 24 h in MDA-MB-468, HCC1937, and SUM149PT cells, as well as in MDA-MB-231 cells. Cleavage of PARP, an indicator of apoptosis, also increased significantly in all tested cell lines after triple combination treatment (Fig. 3a). We next determined Annexin V expression in MDA-MB-231, MDA-MB-468, and SUM149PT cells treated with dasatinib alone or in combination at the indicated concentrations for 48 and 72 h. Our results indicated that treatment with the triple combination significantly induced apoptosis in the three tested cell lines in a dose-dependent manner (Fig. 3b, Supplementary Fig S4). We further confirmed the efficacy of dasatinib alone or in combination on cellular apoptosis in vivo using IHC. Levels of cleaved caspase 3^{Asp175} were increased significantly after treatment with the triple combination in xenograft tumor cells, in agreement with our in vitro results. Of note, cleaved caspase 3^{Asp175} staining in

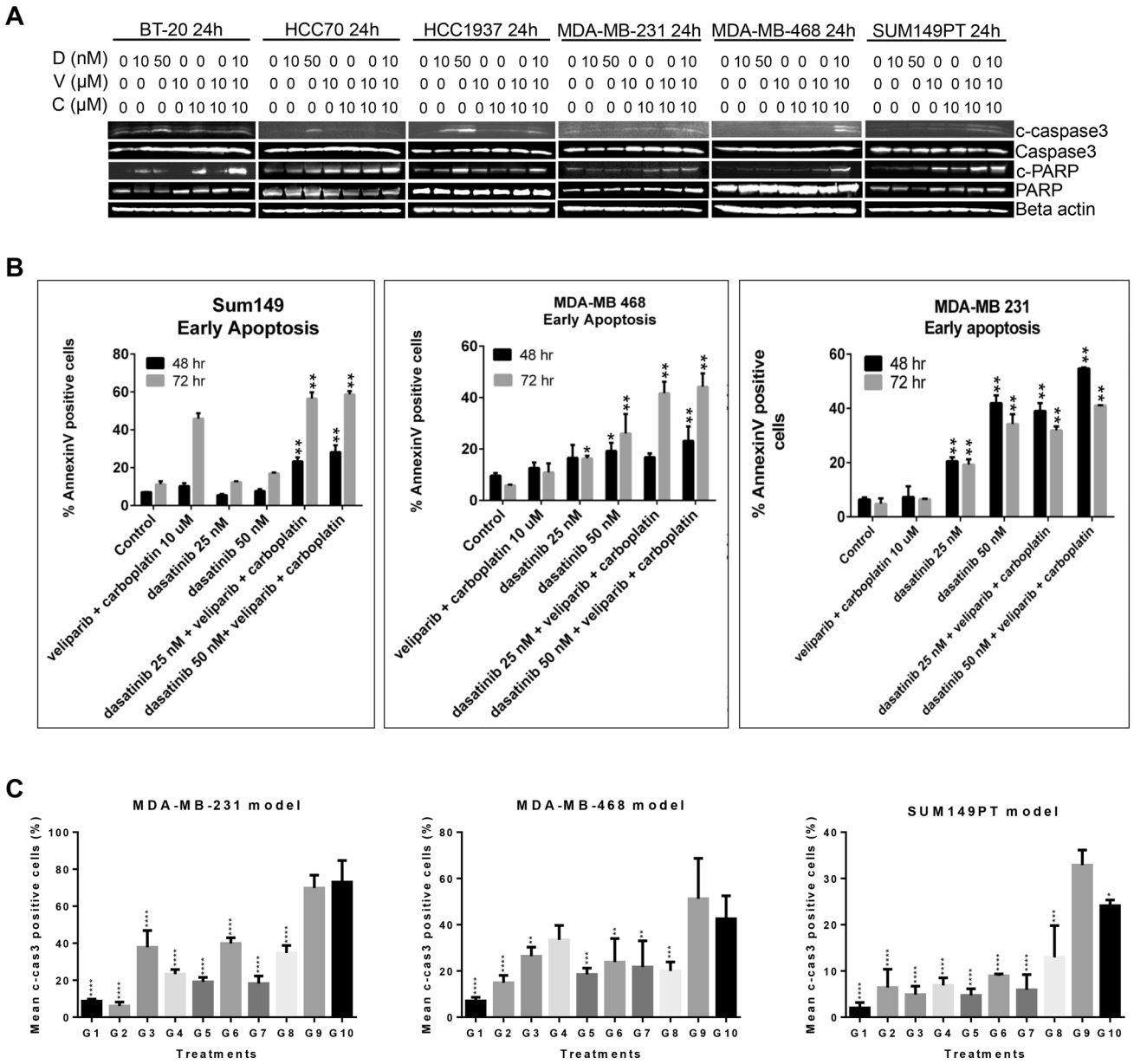

Fig. 3 Effect of dasatinib as a single agent or in combination with veliparib and/or carboplatin on apoptosis in TNBC cells in vitro and in vivo. **a** BT-20, HCC70, HCC1937, MDA-MB-231, MDA-MB-468, and SUM149PT cells were starved in 0.1% FBS medium (phenol red free) for 4 h and treated with dasatinib (10 or 50 nM) as a single agent or in combination with veliparib (10 μM) and/or carboplatin (10 μM) for 24 h. Whole cell lysates were immunoblotted with anti-caspase 3, cleaved anti-caspase 3^{Asp175}, anti-PARP, and cleaved anti-$PARP^{Asp214}$ antibodies. Beta-actin was used as a loading control. **b** Effect of dasatinib as a single agent or in combination with veliparib and/or carboplatin on the apoptotic (early) response analyzed using IHC with anti-Annexin V/7AAD antibodies in MDA-MB-231, MDA-MB-468, and SUM149PT cells. Cells were treated for 48 and 72 h, released, rinsed, and placed in Annexin V binding buffer. Cells were labeled with Annexin V–PE and 7AAD for analysis. Data as means ± SEM (*$P < 0.05$; **$P < 0.005$; two-Way ANOVA). **c** In MDA-MB-231, MDA-MB-468, and SUM149PT xenograft tumor tissues, the expression status of cleaved caspase 3 was determined by IHC. After quantification, the mean percentage of positive cells of cleaved caspase 3 from 4 high-power (× 400) fields is shown graphically, and the bar is SD ($n = 4$). ** $p < 0.005$; ***, $p < 0.001$; ****, $p < 0.0001$ compared the mean of each group with the mean of group 9 (triple combination) by one-way ANOVA followed by Turkey's post hoc test

MDA-MB-231 cells treated with triple combination shows largely extracellular, which is not seen in the other tumor models. The possible cause of this result might be antigen pervasion induced by membrane fragmentation followed by blebbing process during cell apoptosis or necrosis [26] (Fig. 3c, Supplementary Fig S2c).

Combination of dasatinib and veliparib plus carboplatin affects rates of cell cycle progression

To examine if the effects of dasatinib alone or in combination on growth inhibition were the result of altered rates of cell cycle progression, cells were treated and protein lysates were probed for the key cell cycle regulator, cyclin D1, and the cyclin-dependent kinase inhibitor, $p27^{Kip1}$. Decreased expression levels of cyclin D1 were observed in BT-20, HCC1937, MDA-MB-231, MDA-MB-468, and SUM149PT cells after treatment with triple combination, whereas there was no change in cyclin D1 levels in HCC70 cells (Fig. 4a). Increased $p27^{Kip1}$ expression was observed in HCC70, HCC1937, MDA-MB-231, and SUM149PT cells after treatment with the triple combination. There was no change in BT-20 or MDA-MB-468 cells (Fig. 4a). IHC was performed using anti-cyclin D1 antibodies on xenograft tumors indicating that treatment with the triple combination led to the most effective reduction in cyclin D1 levels (Fig. 4b, Supplementary Fig S2**d**).

Combination of dasatinib and veliparib plus carboplatin reduces tube formation in HUVEC cells

Angiogenesis is a multistep process that includes tube formation of endothelial cells. To evaluate the effects of dasatinib as a single agent or in combination with veliparib and/or carboplatin on tumor angiogenesis, the tube formation experiment using HUVEC cells was conducted. After a 6-h incubation with a single agent or drug combinations, capillary-like tubular structures decreased and cell death increased compared with the no treatment controls (Fig. 5a). We next evaluated the degree of tumor angiogenesis using IHC on xenograft tumors. Tumors treated with triple combination exhibited a marked decrease in CD31 expression (Fig. 5b, Supplementary Fig. S2h).

Combination of dasatinib with veliparib and carboplatin is the most effective treatment at inhibiting xenograft tumor growth

KRAS/BRAF-mutated MDA-MB-231, *PTEN* null MDA-MB-468, and *BRCA*-mutated and *PTEN* null SUM149PT xenograft tumors (~200 mm^3) were established in nude mice to determine the antitumor effect of dasatinib, veliparib, or carboplatin alone or in combinations on tumor growth

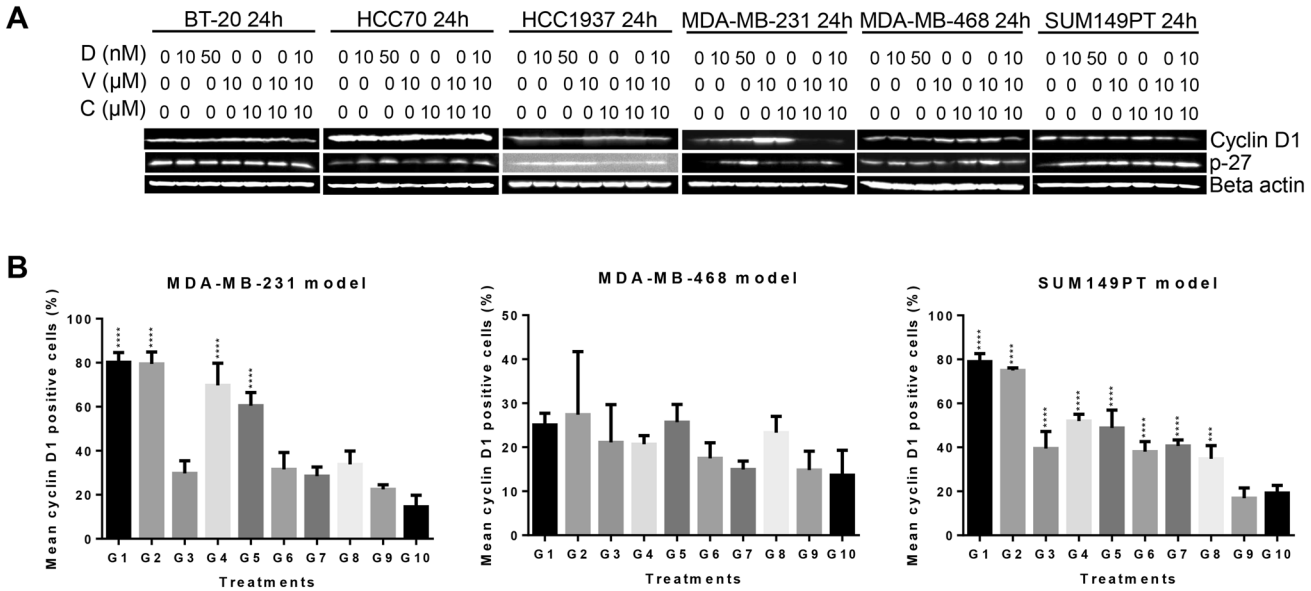

Fig. 4 Effect of dasatinib as a single agent or in combination with veliparib and/or carboplatin on the cell cycle in TNBC cells in vitro and in vivo. **a** BT-20, HCC70, HCC1937, MDA-MB-231, MDA-MB-468, and SUM149PT cells were starved in 0.1% FBS medium (phenol red free) for 4 h and treated with dasatinib (10 or 50 nM) as a single agent or in combination with veliparib (10 μM) and/or carboplatin (10 μM) for 24 h. Whole cell lysates were immunoblotted using anti-cyclin D1 and anti-$P27^{Kip1}$ antibodies. Beta-actin was used as a loading control. **b** In MDA-MB-231, MDA-MB-468, and SUM149PT xenograft tumor tissues, the expression status of cyclin D1 was determined by IHC. After quantification, the mean percentage of positive cells of cyclin D1 staining from 4 high-power (× 400) fields is shown graphically, and the bar is SD ($n=4$). ***, $p<0.001$; ****, $p<0.0001$ compared the mean of each group with the mean of group 9 (triple combination) by one-way ANOVA followed by Turkey's post hoc test

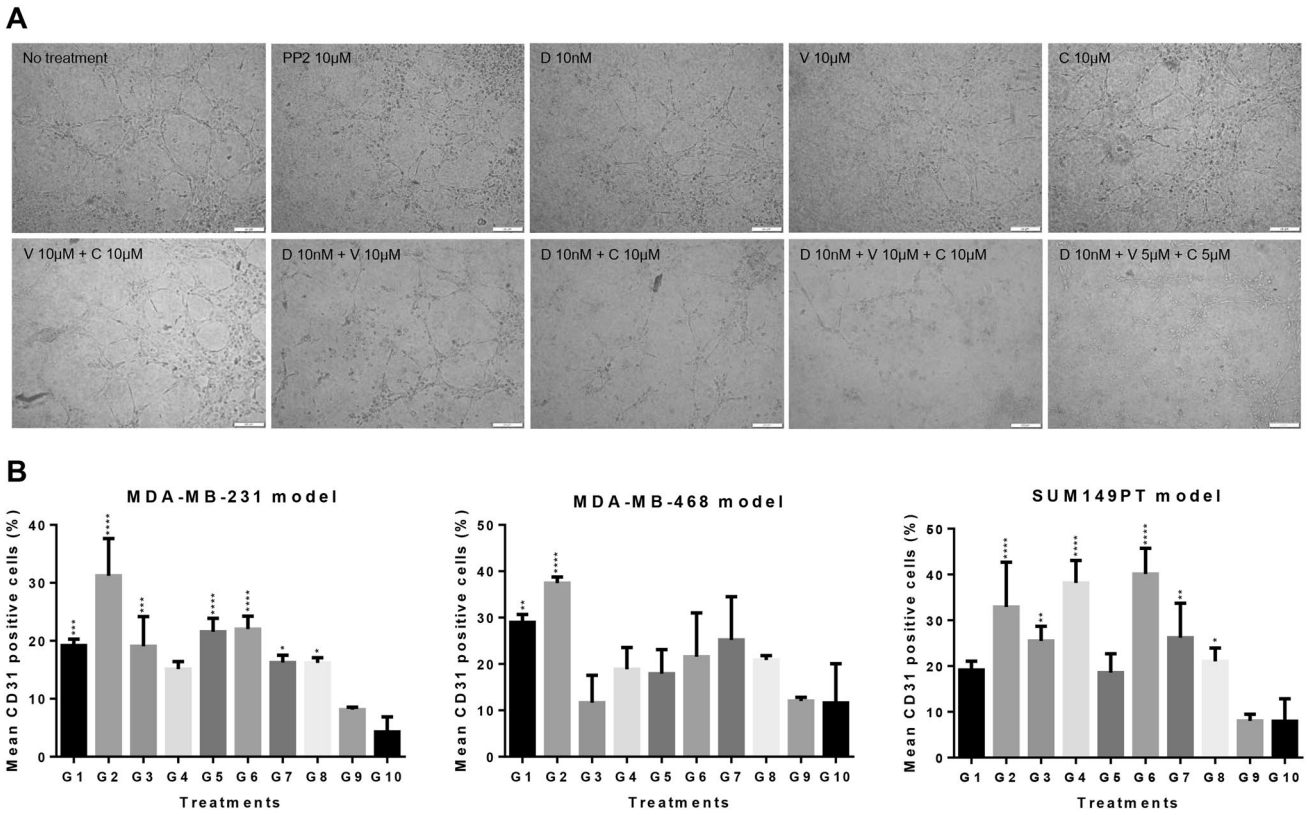

Fig. 5 Effects of dasatinib as a single agent or in combination with veliparib and/or carboplatin on angiogenesis in vitro and in vivo. **a** Effect of dasatinib as a single agent or in combination with veliparib and/or carboplatin on the ability of HUVECs to form capillary-like tubes on matrigel. Cells were seeded onto matrigel and treated for 6 h before representative pictures were taken. The scale bar denotes 200 μm. **b** In MDA-MB-231, MDA-MB-468, and SUM149PT xenograft tumor tissues, the expression status of CD31 was determined by IHC. After quantification, the mean percentage of positive cells of CD31 staining from 4 high-power (× 400) fields is shown graphically, and the bar is SD ($n=4$). *, $p<0.05$; ** $p<0.005$; ***, $p<0.001$; ****, $p<0.0001$ compared the mean of each group with the mean of group 9 (triple combination) by one-way ANOVA followed by Turkey's post hoc test

in vivo. Previous studies have reported that dasatinib in the range of 10–50 mg/kg/day in a 21-day period caused tumor regression in xenograft mouse models [27, 28]. Based on previous publications and summary of product characteristics, we chose to use a comparable dose of 12.5 mg/kg/day of dasatinib (3 weeks), 25 mg/kg/bid of veliparib (5 days) and 40 mg/kg of carboplatin (one dose) for our in vivo studies (Fig. 6; Table 2) [27, 29]. Single agents or double combinations significantly inhibited tumor growth as compared with the non-treated group (single agent $p<0.0001$, double combination $p<0.0001$). The triple combination showed the best antitumor efficacy at both doses of dasatinib, compared with veliparib plus carboplatin ($p<0.0001$) or dasatinib alone ($p<0.0001$ in MDA-MB-231 tumors (Fig. 6a, d). In MDA-MB-468 xenograft model, dasatinib alone ($p<0.0001$) or combination of veliparib and carboplatin ($p<0.0001$) or the triple combination ($p<0.0001$) significantly inhibited tumor growth as compared with the non-treated group. The best tumor inhibition result was obtained with the triple combination (at both doses of dasatinib) compared with dasatinib alone ($p<0.003$) or veliparib plus carboplatin ($p<0.0001$) (Fig. 6b, e). In SUM149PT xenograft model, dasatinib alone ($p<0.0001$) or combination of veliparib and carboplatin ($p<0.0001$) or in the triple combination ($p<0.0001$) significantly inhibited tumor growth as compared with the non-treated group, and the triple combination (at both doses of dasatinib) showed the best antitumor efficacy compared with combination of veliparib and carboplatin ($p<0.0001$) or single agent of dasatinib ($p<0.0001$) (Fig. 6c, f). Single agents or combinations were well tolerated in mice with less than 10% body weight loss compared with vehicle controls in all three xenograft models, and no systemic toxicity was observed (Table 2).

Discussion

In this study, we have provided novel evidence that veliparib combined with carboplatin drives Src activation in preclinical models of TNBC. Moreover, we have provided

provocative in vitro and in vivo data indicating the potential for therapeutic efficacy of combining dasatinib (Src inhibitor) with veliparib (PARP inhibitor) plus carboplatin (DNA-damaging agent) in TNBC. This triple combination may reduce treatment resistance by attenuating the unexpected increase in Src activity, which was induced by the combination of veliparib and carboplatin, and enhance therapeutic efficacy in TNBC.

Growing evidence indicates that deregulation of Src is involved in the development and progression of solid tumors. Given that Src inhibitors as single agents have shown limited clinically beneficial effects in solid tumors, we tested whether the Src inhibitor dasatinib combined with veliparib plus carboplatin would provide a better antitumor effect in TNBC tumors with different genetic backgrounds. We observed Src^{Y416} expression in all tested TNBC cell lines, and found that Src^{Y416} expression was inhibited by dasatinib and PP2 dose dependently at 24 and 72 h (Fig. 1a, Supplementary Fig S5), indicating that dasatinib served as a Src inhibitor in TNBC cell lines [16]. Furthermore, we tested (using the MTS assay) if dasatinib as a single agent or in combination with veliparib and carboplatin could affect tumor cell growth and if the combination had a greater effect than as single agents. Our results showed a range of IC_{50} values in TNBC cells, which was consistent with a previous study [30]. Interestingly, the IC_{50} for dasatinib in combination with veliparib and carboplatin was decreased in *BRCA*-mutated and *PTEN* null HCC1937, SUM149PT, and *PTEN* null HCC70 cells; however, the combination of agents did not enhance the sensitivity of *PIK3CA*-mutated BT-20 or *PTEN* null MDA-MB-468 cells to dasatinib. Thus, other factors may mediate sensitivity of Src inhibition on proliferation to dasatinib alone or in combinations in TNBC cells.

Given the differential responses observed among the different oncogenic drivers, we next analyzed pathway signaling responses to define mechanisms of response. Surprisingly, we observed increased activity in the Src^{Y416} pathway in response to the combination of veliparib with carboplatin in *PTEN* null HCC70, MDA-MB-468, and *BRCA*-mutated and *PTEN* null HCC1937 cells, as well as in *KRAS/BRAF*-mutated MDA-MB-231 cells, which has not been reported to date. IHC of tumors treated with dasatinib alone exhibited a significant decrease in p-Src^{Y416} expression in all tested models; the double combination of dasatinib and carboplatin also induced a significant inhibition of p-Src^{Y416} expression in MDA-MB-231 tumor cells, with greater decreases in p-Src^{Y416} expression observed using the triple combination in all three xenograft models. Furthermore, increases in p-Src^{Y416} expression also occurred in MDA-MB-231 tumor cells. Our finding is a particularly important observation because increased Src activity may affect the efficacy of veliparib combined with carboplatin in the treatment of TNBC. This could at least in part explain why over 40% of TNBC patients receiving the combination of veliparib and carboplatin did not have a pCR in the I-SPY 2 trial [15]. Thus, it is conceivable that the use of the combination of dasatinib with veliparib plus carboplatin would provide a better therapeutic outcome. This triple combination may reduce treatment resistance by attenuating the increased Src activity induced by veliparib and carboplatin.

Our results showed that the triple combination completely blocked colony formation in *BRCA*-mutated and *PTEN* null HCC1937, *KRAS/BRAF*-mutated MDA-MB-231, and *PTEN* null MDA-MB-468, as well as *BRCA*-mutated and *PTEN* null SUM149PT cells. In contrast, even though *PIK3CA*-mutated BT-20 and *PTEN* null HCC70 cell lines showed an enhanced sensitivity to the triple combination, the combination therapy did not completely eliminate colony formation. Src is upstream of the AKT/mTOR and MAPK pathways and has been shown to play a role in mediating activation of the PI3K pathway [31, 32]. Cells treated with the triple combination caused a decrease in p-AKT^{T308} and p-AKT^{S473} expression in *BRCA*-mutated and *PTEN* null SUM149PT cells, and a decrease in p-AKT^{S473} expression in *BRCA* -mutated and *PTEN* null HCC1937 cells. We also observed an inhibitory effect on p-S6 $RP^{S235/236}$ and p-$ERK^{T202/T204}$ expression in *KRAS/BRAF*-mutated MDA-MB-231 and *BRCA*-mutated and *PTEN* null SUM149PT cells using the triple combination. Interestingly, the combination of veliparib with carboplatin increased expression of p-AKT^{T308} and p-AKT^{S473} in *KRAS/BRAF*-mutated MDA-MB-231 and *PTEN* null MDA-MB-468 cells.

Importantly, triple combination increased p-AKT^{S473} and p-$ERK^{T202/T204}$ expression in *PIK3CA*-mutated BT-20 cells, which is consistent with our results in the MTS and 3D 'on-top' assays. IHC of Ki-67, p-AKT^{S473}, p-S6 $RP^{S235/236}$, and p-$ERK^{T202/T204}$ indicated that compared with dasatinib alone, or double combinations, the best inhibitory effects were observed following the triple combination in xenograft tumor cells. Unexpectedly, the expression of p-AKT^{S473} showed no change after treatment with the triple combination in the *KRAS/BRAF*-mutated MDA-MB-231 xenograft model, although this was consistent with western blot results. Future studies will need to define the correlation of the triple combination with the mutational landscape and PI3K pathway as well as Src inhibition in TNBC cells.

Taken together, dasatinib combined with veliparib and carboplatin regulated proliferative and survival signaling through Src and downstream effectors including AKT, S6 RP, and ERK. This is consistent with previous work that showed that Src regulates the PI3K pathway through different effectors including PTEN and AKT [33, 34]. However, our in vitro data with the triple combination showed no effect on regulating proliferative/survival signaling in

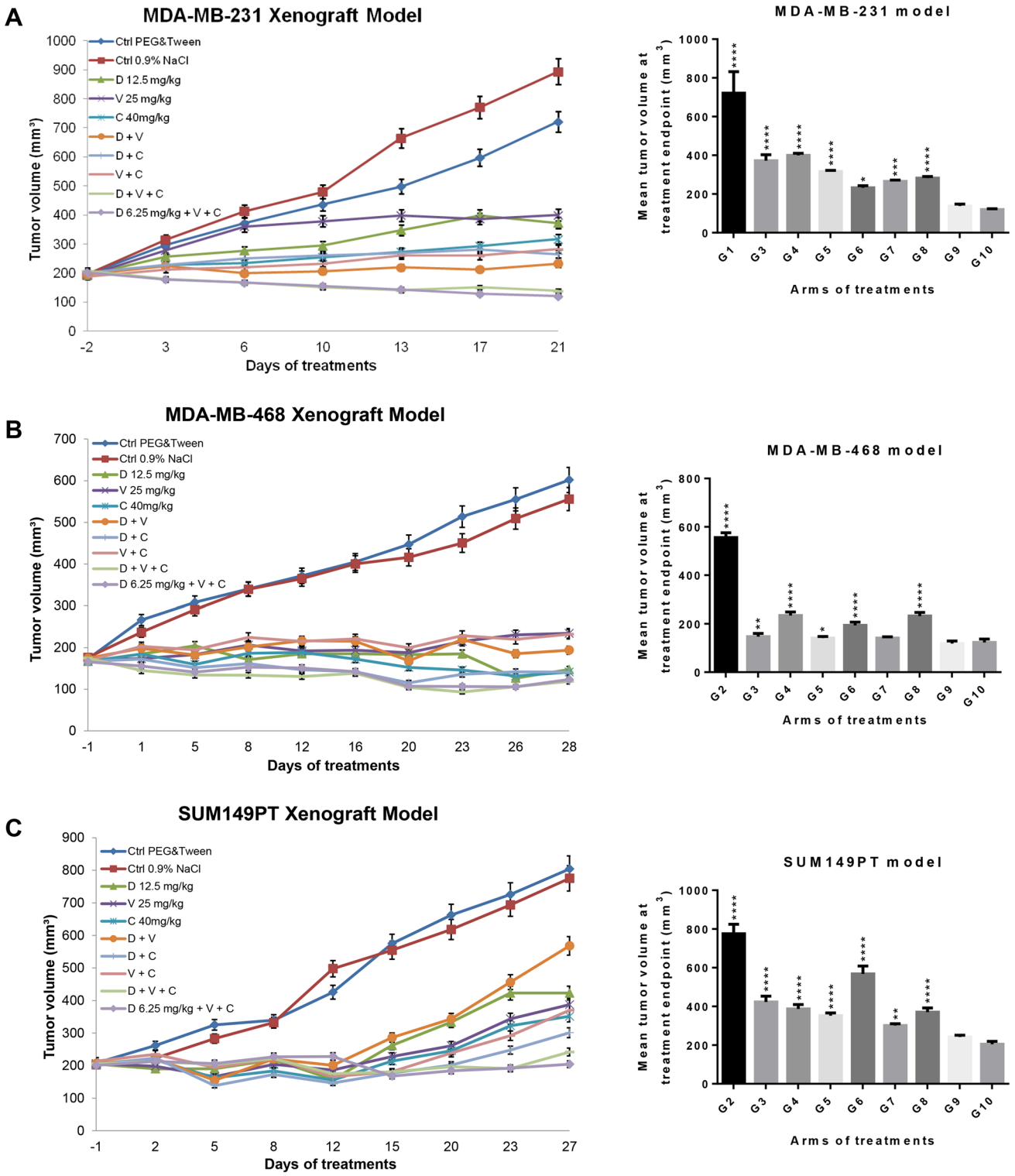

PIK3CA-mutant BT-20 cells, as was shown by Beadnell and colleagues [32].

PARP activity, which was shown to increase after administration of chemotherapy and radiation treatment, underscores the important role of PARP in DDR and DNA repair [35]. Combining the PARP inhibitor with a DNA-damaging agent such as carboplatin is a promising treatment in TNBC, especially in patients without germline BRCA1/2 (gBRCA) mutations [15, 36, 37]. We observed markedly increased PARP cleavage induced by the triple combination in all tested TNBC cells and increased cleaved caspase 3 in *PTEN* null MDA-MB-468, *BRCA*-mutated and *PTEN*

◂**Fig. 6** Dasatinib enhances the antitumor effect of veliparib plus carboplatin in TNBC xenograft models. Immunocompromised female nude (nu/nu) mice were implanted with **a** MDA-MB-231 cells; **b** MDA-MB-468 cells and **c** SUM149PT cells. Mice were treated with ten groups: 1. Vehicle (5.1% PEG 400 and 5.1% Tween 80 in ddH_2O) 100 µl by i.p. once daily, dosing schedule of 5 days of vehicle followed by 2 days off the vehicle. 2. Vehicle (0.9% NaCl, PH 4.0) 50 µl by oral gavage twice daily for 5 days. 3. Dasatinib (D) 12.5 mg/kg, i.p., once daily, dosing schedule of 5 days of dasatinib followed by 2 days off the drug. 4. Veliparib (V) 25 mg/kg, oral gavage, twice daily for 5 days. 5. Carboplatin (C) 40 mg/kg, i.v. one dose at starting day. 6. D (12.5 mg/kg) + V (25 mg/kg). 7. D (12.5 mg/kg) + C (40 mg/kg). 8. V (25 mg/kg) + C (40 mg/kg). 9. D (12.5 mg/kg) + V (25 mg/kg) + C (40 mg/kg). 10. D (6.25 mg/kg) + V (25 mg/kg) + C (40 mg/kg). Tumor volumes were measured twice per week at the indicated time points. Person performing the measurements was blinded to the treatments. **d–f** Statistically significant differences of mean tumor volumes at treatment endpoints ($n = 5$–8 mice/group, see details in Table 2) were analyzed using one-way ANOVA followed by Bonferroni post hoc test (*, $p < 0.05$; ** $p < 0.005$; ***, $p < 0.001$; ****, $p < 0.0001$). Bars in panels **a–e** represent SEM. Control group with smaller mean tumor volume at treatment endpoints of each xenograft model was selected for statistical analysis. None of mice were dropped out from MDA-MB-231 model; one mouse of group 3, group 6, group 7 and group 10 from MDA-MB-468 model were found dead during the experiment for unknown reason, and one mouse of group 10 was killed due to loss of body weight more than 10% from MDA-MB-468 model; one mouse of group 8 was killed due to loss of body weight from SUM149PT model, one mouse of group 3, group 6 and group 10 from SUM149PT model was found dead during the experiment for unknown reason (see Table 2)

null HCC1937, SUM149PT, and *KRAS/BRAF*-mutated MDA-MB-231 cells. Of note, MDA-MB-468 cells showed a high IC_{50} of dasatinib, and combination of agents did not enhance the sensitivity to dasatinib; furthermore, neither veliparib plus carboplatin nor triple combination showed inhibitory effect on p-AKT^{T308}, p-AKT^{S473}, p-S6 $RP^{S235/236}$ or p-$ERK^{T202/T204}$. In contrast, our in vivo results showed significant antitumor activities by dasatinib alone or in combinations. The possible cause of these results might be the antitumor effects mainly through apoptosis which happened in days or weeks in vivo [26].

Interestingly, dasatinib alone at a high dose (50 nM) induced increasing levels of cleaved caspase 3 in *PIK3CA*-mutated BT-20 and *PTEN* null HCC70 cell lines, suggesting that a higher dose of dasatinib in combination with veliparib and carboplatin might have a better effect on apoptosis in these two cell lines. Moreover, Annexin V staining demonstrated better early stage apoptosis caused by the triple combination compared with dasatinib alone or the combination of veliparib and carboplatin in *KRAS/BRAF*-mutated MDA-MB-231, *PTEN* null MDA-MB-468, and *BRCA*-mutated and *PTEN* null SUM149PT cells, whereas single agents and combinations failed to induce an increase in Annexin V-positive cells in *PIK3CA*-mutated BT-20, *PTEN* null HCC70, or *BRCA*-mutated and *PTEN* null HCC1937 cell lines. Furthermore, IHC showed greater cleaved caspase 3 expression induced by the triple combination compared with single agents and double combinations in xenograft tumor cells.

Previous studies demonstrated that Src not only has a role in apoptosis, but is also involved in cell cycle progression [3]. Consistently, our data showed that the triple combination increased $p27^{Kip1}$ in *PTEN* null HCC70, *KRAS/BRAF*-mutated MDA-MB-231, and *BRCA*-mutated and *PTEN* null SUM149PT cells, and decreased cyclin D1 expression in all tested in vitro and in vivo models. Taken together, Src inhibition by dasatinib induced cell cycle arrest and apoptosis and may contribute to the antitumor efficacy observed with the triple combination [38].

In TNBC, pathological angiogenesis occurs at a late stage in tumor proliferation and is associated with invasion and metastasis [39]. Development of agents that inhibit tumor angiogenesis has been an active area of investigation [40]. Src has been shown to play a role in the regulation of tumor angiogenesis [41]. Consistently, IHC results demonstrated a marked decrease in CD31 expression induced by the triple combination in xenograft tumor cells. Our results showed a greater inhibitory effect on tube formation in HUVEC cells by the triple combination compared with single agents and double combinations. Thus, the triple combination may have enhanced the antitumor effect by inhibiting angiogenic cells.

In our xenograft models, the triple combination demonstrated the best antitumor effects compared with single agents or double combinations. Of note, the triple combination, even with dasatinib reduced to half the dose (Group 9, dasatinib 12.5 mg/kg and Group 10, dasatinib 6.25 mg/kg), gave similar antitumor effects. The 6.25 mg/kg was less than what has been used by others in xenograft models [3, 27, 28]. The higher rates of hematologic and nonhematologic toxic effects of veliparib–carboplatin treatment have been reported by the I-SPY 2 investigators that were similar to the toxic effects found in association with carboplatin in the CALGB 40603 trial [15, 42]; a phase I trial also showed a high-grade neutropenia when dasatinib combined with carboplatin in patients with ovarian cancer [21]. To best combine the three agents in our study, we reduced the dose of dasatinib to 6.25 mg/kg/day (convert to human equivalent dose is 0.51 mg/kg/day) and carboplatin to 40 mg/kg (one dose on day 0, convert to human equivalent dose is 120 mg/m^2), as well as scheduled dasatinib 5 days per week and veliparib for total 5 days delivery. Increased systemic toxicity was not observed in our xenograft model when comparing the treated groups with vehicle controls [31]. Furthermore, the triple combination was well tolerated with less than 10% body weight loss compared with vehicle controls in all three xenograft models.

The study had limitations that should be mentioned, including the use of cell line-derived ectopic xenograft models instead of orthotopic model. The different

Table 2 Mean body weight changes of mice

a. MDA-MB-231 model				
Treatment Groups*	Number of mice (*n*; day-1)	Number of mice (*n*; day 21)	Body weight (day-1) (gram ± SEM)	Body weight (day 21) (gram ± SEM)
1	6	6	24.7 ± 0.41	25.9 ± 0.35
2	6	6	25.8 ± 0.26	27.0 ± 0.43
3	6	6	23.7 ± 0.49	25.5 ± 0.22
4	6	6	24.9 ± 0.29	25.6 ± 0.30
5	5	5	24.2 ± 0.22	26.7 ± 0.21
6	6	6	24.2 ± 0.24	25.1 ± 0.23
7	5	5	24.1 ± 0.29	22.3 ± 1.32
8	5	5	24.7 ± 0.31	23.6 ± 0.84
9	5	5	24.2 ± 0.28	23.2 ± 0.48
10	5	5	25.3 ± 0.24	25.8 ± 0.33
b. MDA-MB-468 model				
Treatment Groups*	Number of mice (*n*; day-1)	(*n*; day 28) Number of mice	Body weight (day-1) (gram ± SEM)	Body weight (day 28) (gram ± SEM)
1	8	8	21.1 ± 0.30	23.2 ± 0.34
2	8	8	21.3 ± 0.20	23.3 ± 0.28
3	8	7	22.3 ± 0.39	22.0 ± 0.23
4	8	8	20.5 ± 0.21	22.5 ± 0.25
5	8	8	21.1 ± 0.26	22.0 ± 0.28
6	7	6	22.0 ± 0.28	23.0 ± 0.40
7	8	7	21.0 ± 0.17	21.1 ± 0.41
8	8	8	21.7 ± 0.22	23.0 ± 0.33
9	8	8	20.5 ± 0.18	20.5 ± 0.36
10	8	6	21.5 ± 0.26	22.8 ± 0.38
c. SUM149PT model				
Treatment Groups*	Number of mice (*n*; day-1)	Number of mice (*n*; day 27)	Body weight (day -1) (gram ± SEM)	Body weight (day 27) (gram ± SEM)
1	8	8	22.5 ± 0.14	24.7 ± 0.18
2	8	8	22.6 ± 0.56	24.6 ± 0.73
3	8	7	20.0 ± 0.56	24.7 ± 0.85
4	8	8	21.3 ± 0.49	20.0 ± 0.62
5	8	8	21.2 ± 0.59	23.1 ± 0.51
6	8	7	22.3 ± 0.53	25.1 ± 0.50
7	8	8	21.5 ± 0.46	22.8 ± 0.89
8	8	7	22.1 ± 0.85	22.8 ± 0.89
9	8	8	20.0 ± 0.70	23.8 ± 0.83
10	8	7	21.8 ± 0.76	23.7 ± 0.94

*See details of treatment groups on the legend of Fig. 6

SEM standard error of the mean

microenvironments, particularly the vascular system of the tumor may impact tumor growth and therapeutic result [43]. Choosing more appropriate models in future studies should be considered. Another limitation relates to the lack of evaluations on toxic effects of the treatments. Although we measured the body weight and monitored the behaviors of the mice, more research approaches on treatment toxicities should be considered in future studies to ensure the feasible, safe and effective antitumor treatment strategies.

To our knowledge, we are the first to provide preclinical evidence that the combination of veliparib and carboplatin induces increased Src activity. This is a particularly

important observation because increased Src activity may affect the efficacy of veliparib combined with carboplatin in TNBC. Furthermore, the results from our in vitro and in vivo studies demonstrate that addition of dasatinib attenuates the overexpression of Src signaling and enhances antitumor activity of veliparib plus carboplatin in TNBC cells. This study provides the preclinical basis for undertaking a clinical trial using this novel triple combination of dasatinib with veliparib plus carboplatin in TNBC.

Acknowledgements We sincerely thank National Cancer Institute for providing us drugs and we highly appreciate Avera Cancer Institute for supporting this study.

Author contributions YS carried out the majority of the in vitro and in vivo experiments and drafted the article. XL performed in vitro and in vivo experiments and contributed to several figures. JA conceived critical experiments of cellular apoptosis. PY helped with Statistical analysis. CW participated in coordination of the study. MA helped draft the manuscript. BL-J and YS conceived the study and supervised all experiments. All authors read and approved the final article.

Funding This study was supported by Avera Cancer Institute.

Compliance with ethical standards

Conflict of interest Casey Williams is a consultant of Takeda, and he has received funding from Takeda, Tesaro and Pfizer. Brian Leyland-Jones is a consultant of Takeda and Tesaro. The other authors declare that they have no conflict of interest.

Ethical approval All applicable international, national, and/or institutional guidelines for the care and use of animals were followed.

References

1. DeSantis C, Siegel R, Bandi P (2011) Jemal A (2011) Breast cancer statistics. CA Cancer J Clin 61(6):409–418
2. Miller KD, Siegel RL, Lin CC, Mariotto AB, Kramer JL, Rowland JH, Stein KD, Alteri R, Jemal A (2016) Cancer treatment and survivorship statistics. CA Cancer J Clin 66(4):271–289
3. Qian XL, Zhang J, Li PZ, Lang RG, Li WD, Sun H, Liu FF, Guo XJ, Gu F, Fu L (2017) Dasatinib inhibits c-src phosphorylation and prevents the proliferation of Triple-Negative Breast Cancer (TNBC) cells which overexpress Syndecan-Binding Protein (SDCBP). PLoS One 12(1):e0171169
4. Sulaiman A, Wang L (2017) Bridging the divide: preclinical research discrepancies between triple-negative breast cancer cell lines and patient tumors. Oncotarget 8(68):113269–113281
5. Bianchini G, Balko JM, Mayer IA, Sanders ME, Gianni L (2016) Triple-negative breast cancer: challenges and opportunities of a heterogeneous disease. Nat Rev Clin Oncol 13(11):674–690
6. Lee A, Djamgoz MBA (2018) Triple negative breast cancer: Emerging therapeutic modalities and novel combination therapies. Cancer Treat Rev 62:110–122
7. Roy R, Chun J, Powell SN (2011) BRCA1 and BRCA2: different roles in a common pathway of genome protection. Nat Rev Cancer 12(1):68–78
8. Tahara M, Inoue T, Sato F, Miyakura Y, Horie H, Yasuda Y, Fujii H, Kotake K, Sugano K (2014) The use of Olaparib (AZD2281) potentiates SN-38 cytotoxicity in colon cancer cells by indirect inhibition of Rad51-mediated repair of DNA double-strand breaks. Mol Cancer Ther 13(5):1170–1180
9. Farmer H, McCabe N, Lord CJ, Tutt AN, Johnson DA, Richardson TB, Santarosa M, Dillon KJ, Hickson I, Knights C et al (2005) Targeting the DNA repair defect in BRCA mutant cells as a therapeutic strategy. Nature 434(7035):917–921
10. Tutt A, Robson M, Garber JE, Domchek SM, Audeh MW, Weitzel JN, Friedlander M, Arun B, Loman N, Schmutzler RK et al (2010) Oral poly(ADP-ribose) polymerase inhibitor olaparib in patients with BRCA1 or BRCA2 mutations and advanced breast cancer: a proof-of-concept trial. Lancet 376(9737):235–244
11. Robson M, Im SA, Senkus E, Xu B, Domchek SM, Masuda N, Delaloge S, Li W, Tung N, Armstrong A et al (2017) Olaparib for metastatic breast cancer in patients with a Germline BRCA Mutation. N Engl J Med 377(6):523–533
12. De P, Sun Y, Carlson JH, Friedman LS, Leyland-Jones BR, Dey N (2014) Doubling down on the PI3 K-AKT-mTOR pathway enhances the antitumor efficacy of PARP inhibitor in triple negative breast cancer model beyond BRCA-ness. Neoplasia 16(1):43–72
13. Basourakos SP, Li L, Aparicio AM, Corn PG, Kim J, Thompson TC (2017) Combination platinum-based and DNA damage response-targeting cancer therapy: evolution and future directions. Curr Med Chem 24(15):1586–1606
14. Gampenrieder SP, Rinnerthaler G, Greil R (2017) SABCS 2016: systemic therapy for metastatic breast cancer. Memo 10(2):86–89
15. Rugo HS, Olopade OI, DeMichele A, Yau C, Veer LJ, Buxton MB, Hogarth M, Hylton NM, Paoloni M, Perlmutter J et al (2016) Adaptive randomization of veliparib-carboplatin treatment in breast cancer. N Engl J Med 375(1):23–34
16. Pichot CS, Hartig SM, Xia L, Arvanitis C, Monisvais D, Lee FY, Frost JA, Corey SJ (2009) Dasatinib synergizes with doxorubicin to block growth, migration, and invasion of breast cancer cells. Br J Cancer 101(1):38–47
17. Han MW, Ryu IS, Lee JC, Kim SH, Chang HW, Lee YS, Lee S, Kim SW, Kim SY (2018) Phosphorylation of PI3 K regulatory subunit p85 contributes to resistance against PI3 K inhibitors in radioresistant head and neck cancer. Oral Oncol 78:56–63
18. Ibrahim YH, Garcia-Garcia C, Serra V, He L, Torres-Lockhart K, Prat A, Anton P, Cozar P, Guzman M, Grueso J et al (2012) PI3 K inhibition impairs BRCA1/2 expression and sensitizes BRCA-proficient triple-negative breast cancer to PARP inhibition. Cancer Discov 2(11):1036–1047
19. Tarpley M, Abdissa TT, Johnson GL, Scott JE (2014) Bosutinib reduces the efficacy of Dasatinib in triple-negative breast cancer cell lines. Anticancer Res 34(4):1629–1635
20. Finn RS, Bengala C, Ibrahim N, Roche H, Sparano J, Strauss LC, Fairchild J, Sy O, Goldstein LJ (2011) Dasatinib as a single agent in triple-negative breast cancer: results of an open-label phase 2 study. Clin Cancer Res 17(21):6905–6913
21. Secord AA, Teoh DK, Barry WT, Yu M, Broadwater G, Havrilesky LJ, Lee PS, Berchuck A, Lancaster J, Wenham RM (2012) A phase I trial of dasatinib, an SRC-family kinase inhibitor, in combination with paclitaxel and carboplatin in patients with advanced or recurrent ovarian cancer. Clin Cancer Res 18(19):5489–5498
22. Sun Y, Dey N, Brammer M, De P, Leyland-Jones B (2013) Bevacizumab confers additional advantage to the combination of trastuzumab plus pertuzumab in trastuzumabrefractory breast cancer model. Cancer Chemother Pharmacol 72(4):733–745

23. Lee GY, Kenny PA, Lee EH, Bissell MJ (2007) Three-dimensional culture models of normal and malignant breast epithelial cells. Nat Methods 4(4):359–365
24. Serrels A, Macpherson IR, Evans TR, Lee FY, Clark EA, Sansom OJ, Ashton GH, Frame MC, Brunton VG (2006) Identification of potential biomarkers for measuring inhibition of Src kinase activity in colon cancer cells following treatment with dasatinib. Mol Cancer Ther 5(12):3014–3022
25. Lieser SA, Shaffer J, Adams JA (2006) SRC tail phosphorylation is limited by structural changes in the regulatory tyrosine kinase Csk. J Biol Chem 281(49):38004–38012
26. Galluzzi L, Bravo-San Pedro JM, Vitale I, Aaronson SA, Abrams JM, Adam D, Alnemri ES, Altucci L, Andrews D, Annicchiarico-Petruzzelli M et al (2015) Essential versus accessory aspects of cell death: recommendations of the NCCD 2015. Cell Death Differ 22(1):58–73
27. Sen B, Peng S, Woods DM, Wistuba I, Bell D, El-Naggar AK, Lai SY, Johnson FM (2012) STAT5A-mediated SOCS2 expression regulates Jak2 and STAT3 activity following c-Src inhibition in head and neck squamous carcinoma. Clin Cancer Res 18(1):127–139
28. Morton JP, Karim SA, Graham K, Timpson P, Jamieson N, Athineos D, Doyle B, McKay C, Heung MY, Oien KA et al (2010) Dasatinib inhibits the development of metastases in a mouse model of pancreatic ductal adenocarcinoma. Gastroenterology 139(1):292–303
29. Kamath AV, Wang J, Lee FY, Marathe PH (2008) Preclinical pharmacokinetics and in vitro metabolism of dasatinib (BMS-354825): a potent oral multi-targeted kinase inhibitor against SRC and BCR-ABL. Cancer Chemother Pharmacol 61(3):365–376
30. Finn RS, Dering J, Ginther C, Wilson CA, Glaspy P, Tchekmedyian N, Slamon DJ (2007) Dasatinib, an orally active small molecule inhibitor of both the src and abl kinases, selectively inhibits growth of basal-type/"triple-negative" breast cancer cell lines growing in vitro. Breast Cancer Res Treat 105(3):319–326
31. Mishall KM, Beadnell TC, Kuenzi BM, Klimczak DM, Supert-Furga G, Rix U, Schweppe RE (2017) Sustained activation of the AKT/mTOR and MAP kinase pathways mediate resistance to the Src inhibitor, dasatinib, in thyroid cancer. Oncotarget 8(61):103014–103031
32. Beadnell TC, Nassar KW, Rose MM, Clark EG, Danysh BP, Hofmann MC, Pozdeyev N, Schweppe RE (2018) Src-mediated regulation of the PI3 K pathway in advanced papillary and anaplastic thyroid cancer. Oncogenesis 7(2):23
33. Lu Y, Yu Q, Liu JH, Zhang J, Wang H, Koul D, McMurray JS, Fang X, Yung WK, Siminovitch KA et al (2003) Src family protein-tyrosine kinases alter the function of PTEN to regulate phosphatidylinositol 3-kinase/AKT cascades. J Biol Chem 278(41):40057–40066
34. Zhao Y, Scott A, Zhang P, Hao Y, Feng X, Somasundaram S, Khalil AM, Willis J, Wang Z (2017) Regulation of paxillin-p130-PI3 K-AKT signaling axis by Src and PTPRT impacts colon tumorigenesis. Oncotarget 8(30):48782–48793
35. Skidmore CJ, Davies MI, Goodwin PM, Halldorsson H, Lewis PJ, Shall S, Zia'ee AA (1979) The involvement of poly(ADP-ribose) polymerase in the degradation of NAD caused by gamma-radiation and *N*-methyl-*N*-nitrosourea. Eur J Biochem 101(1):135–142
36. Owonikoko TK, Zhang G, Deng X, Rossi MR, Switchenko JM, Doho GH, Chen Z, Kim S, Strychor S, Christner SM et al (2014) Poly (ADP) ribose polymerase enzyme inhibitor, veliparib, potentiates chemotherapy and radiation in vitro and in vivo in small cell lung cancer. Cancer Med 3(6):1579–1594
37. Bartelink IH, Prideaux B, Krings G, Wilmes L, Lee PRE, Bo P, Hann B, Coppe JP, Heditsian D, Swigart-Brown L et al (2017) Heterogeneous drug penetrance of veliparib and carboplatin measured in triple negative breast tumors. BCR 19(1):107
38. Le XF, Mao W, Lu Z, Carter BZ, Bast RC Jr (2010) Dasatinib induces autophagic cell death in human ovarian cancer. Cancer 116(21):4980–4990
39. Chhibber-Goel J, Gaur A, Singhal V, Parakh N, Bhargava B, Sharma A (2016) The complex metabolism of trimethylamine in humans: endogenous and exogenous sources. Expert Rev Mol Med 18:e8
40. Ribatti D, Nico B, Ruggieri S, Tamma R, Simone G, Mangia A (2016) Angiogenesis and antiangiogenesis in triple-negative breast cancer. Transl Oncol 9(5):453–457
41. Cavalloni G, Peraldo-Neia C, Sarotto I, Gammaitoni L, Migliardi G, Soster M, Marchio S, Aglietta M, Leone F (2012) Antitumor activity of Src inhibitor saracatinib (AZD-0530) in preclinical models of biliary tract carcinomas. Mol Cancer Ther 11(7):1528–1538
42. Sikov WM, Berry DA, Perou CM, Singh B, Cirrincione CT, Tolaney SM, Kuzma CS, Pluard TJ, Somlo G, Port ER et al (2015) Impact of the addition of carboplatin and/or bevacizumab to neoadjuvant once-per-week paclitaxel followed by dose-dense doxorubicin and cyclophosphamide on pathologic complete response rates in stage II to III triple-negative breast cancer: CALGB 40603 (Alliance). J Clin Oncol 33(1):13–21
43. Fleming JM, Miller TC, Meyer MJ, Ginsburg E, Vonderhaar BK (2010) Local regulation of human breast xenograft models. J Cell Physiol 224(3):795–806